arXiv:1405.0245v1 [cond-mat.stat-mech] 1 May 2014

Maximally dense packings of two-dimensional convex and concave noncircular particles

Steven Atkinson
Department of Mechanical and Aerospace Engineering, Princeton University, Princeton, New Jersey 08544, USA

Yang Jiao
Princeton Institute for the Science and Technology of Materials, Princeton University, Princeton, New Jersey 08544, USA

Salvatore Torquato
Department of Chemistry, Department of Physics, Princeton Center for Theoretical Science, Program of Applied and Computational Mathematics, Princeton Institute for the Science and Technology of Materials, Princeton University, Princeton New Jersey 08544, USA

(Dated: May 2, 2014)

Dense packings of hard particles have important applications in many fields, including condensed matter physics, discrete geometry and cell biology. In this paper, we employ a stochastic search implementation of the Torquato-Jiao Adaptive-Shrinking-Cell (ASC) optimization scheme [Nature (London) **460**, 876 (2009)] to find maximally dense particle packings in d-dimensional Euclidean space $\mathbb{R}^d$. While the original implementation was designed to study spheres and convex polyhedra in $d \geq 3$, our implementation focuses on $d = 2$ and extends the algorithm to include both concave polygons and certain complex convex or concave non-polygonal particle shapes. We verify the robustness of this packing protocol by successfully reproducing the known putative optimal packings of congruent copies of regular pentagons and octagons, then employ it to suggest dense packing arrangements of congruent copies of certain families of concave crosses, convex and concave curved triangles (incorporating shapes resembling the Mercedes-Benz logo), and "moon-like" shapes. Analytical constructions are determined subsequently to obtain the densest known packings of these particle shapes. For the examples considered, we find that the densest packings of both convex and concave particles with central symmetry are achieved by their corresponding optimal Bravais lattice packings; for particles lacking central symmetry, the densest packings obtained are non-lattice periodic packings, which are consistent with recently-proposed general organizing principles for hard particles. Moreover, we find that the densest known packings of certain curved triangles are periodic with a four-particle basis, and we find that the densest known periodic packings of certain moon-like shapes possess no inherent symmetries. Our work adds to the growing evidence that particle shape can be used as a tuning parameter to achieve a diversity of packing structures.

PACS numbers: 61.50.Ah, 05.20.Jj

I. INTRODUCTION

The problem of packing nonoverlapping particles in d-dimensional Euclidean space $\mathbb{R}^d$ has been of interest in discrete mathematics and geometry for centuries. One overarching aim is to ascertain organizing principles that govern the nature of dense packings of various shapes [1] in order to better understand many natural phenomena, including liquid, glassy and crystalline states of matter [2–5]; heterogeneous materials [4]; crystalline polymers [6, 7]; and biological systems [8–10]; to name a few. In two dimensions, the packing of hard particles has implications for understanding the behavior and structures found in thin films [11], adsorption of molecules on substrates [12, 13], and the organization of epithelial cells [14, 15].

In the two-dimensional Euclidean plane $\mathbb{R}^2$, considerable effort has been devoted to study and characterize packings (roughly speaking, large collections of nonoverlapping particles), especially of congruent copies of convex particles [16–21]. Perhaps the simplest characteristic of a packing is its packing density, ϕ, which is, intuitively speaking, the fraction of the plane covered by the particles. It is well known that the triangular lattice is the densest packing of congruent circles, and its packing density is $\phi = \pi/\sqrt{12} = 0.906899\ldots$ [22]. Other simple two-dimensional shapes that have been studied include the class of regular polygons and related variations. For example, it is known that the densest packing of congruent regular octagons is the optimal Bravais lattice packing with $\phi = \left[4(3-\sqrt{2})\right]/7 = 0.906163\ldots$. When the corners of the octagon are all appropriately "smoothed" into hyperbolic curves, the resulting "smoothed octagon" is conjectured to possess the lowest optimal packing density among all convex, centrally-symmetric particle shapes, with $\phi = (8 - 4\sqrt{2} - \ln 2)/(2\sqrt{2} - 1) = 0.902414\ldots$ [23]. Another simple yet interesting case is the regular pentagon, which has a putative maximum packing density

of $\phi = (5 - \sqrt{5})/3 = 0.921311\ldots$, given by its densest (non-Bravais) double-lattice packing [24–27].

Generally, it has been shown independently by both Fejes Tóth [18] and Rogers [17] that the densest packing of congruent copies of any convex, two-dimensional shape possessing central symmetry is achieved by a lattice structure. Fejes Tóth [28] and Mahler [29] also proved that such a construction must be able to achieve a packing density of at least $\phi = \sqrt{3}/2 = 0.866025\ldots$ for any convex shape. Moreover, Kuperberg and Kuperberg showed that, for any convex shape (with or without central symmetry), a double-lattice packing may be constructed, also with $\phi \geq \sqrt{3}/2$, and conjectured that the densest double-lattice packing realizes the maximum packing density for shapes such as regular pentagons and heptagons while asking if this might extend to all regular polygons with an odd number of sides [25].

In the present work, we use a two-dimensional stochastic search implementation of the Torquato-Jiao Adaptive Shrinking Cell (ASC) packing method, originally implemented in three and higher dimensions in Refs. [30–32], to generate the densest known packings of a variety of nontrivial convex and concave noncircular particles. The ASC scheme generates dense packings by rearranging a nonoverlapping configuration of particles within a periodic Fundamental Cell (FC) whilst decreasing its volume to increase the packing density. Our current implementation of the ASC scheme expands upon the previous one by detecting overlaps between any concave polygons and certain smoothly shaped convex and concave nonspherical particles. This allows us to readily investigate dense packings of a wide spectrum of nontrivial nonspherical particles in the plane that exhibit unique packing behaviors.

In this paper, we study the dense packing behavior of several families of noncircular particle shapes including so-called "fat crosses", convex and concave "curved triangles" (incorporating shapes resembling the Mercedes-Benz logo), and "moon-like" shapes. We then use the results of the ASC algorithm to inform analytical constructions of the densest known packings of those particle shapes considered, recovering several well-known results, then moving onward to study other particle shapes. Specifically, we find that the densest packings of certain curved triangles are periodic with a four-particle basis. Also, we find that the densest periodic packings of certain moon-like shapes possess no inherent symmetries. Our work adds to the growing evidence that particle shape can be used as a tuning parameter to achieve a diversity of packing structures.

The rest of this paper is organized as follows: in Sec. II, we will introduce the mathematical definitions that are necessary for a rigorous treatment of the packing problem; in Sec. III, we review the ASC scheme and discuss our contributions to the method; in Sec. IV, we introduce the particle shapes whose packing behavior we have studied; and in Sec. V, we discuss a number of results in packing congruent copies of both well-known and other particle shapes. We then offer conclusions and plans for future work. In addition, an appendix includes some additional numerical results, and the *Supplemental Material* contains mathematical details for many of the packing structures presented in this work[33].

II. DEFINITIONS

In order to make precise the problem that will be addressed, we introduce some mathematical definitions. First, we define a particle, S, to be a closed, simply-connected set in $\mathbb{R}^2$ that may be either concave or convex. The boundary of the set is denoted as Γ. A special case of convexity is strict convexity, denoting a convex boundary that contains no line segments. The area of S is denoted by a_1, and we will henceforth assume that this quantity is bounded.

Given two linearly independent (column) vectors $\boldsymbol{\lambda}_1$ and $\boldsymbol{\lambda}_2$, the *lattice* generated by $\boldsymbol{\lambda}_1$ and $\boldsymbol{\lambda}_2$ is defined as the set $\{i\boldsymbol{\lambda}_1 + j\boldsymbol{\lambda}_2 \; \forall i, j \in \mathbb{Z}\}$. A packing, $\mathcal{P}$ is defined as a collection of particles $\{S_i\}$ whose interiors are mutually disjoint. If all members of $\mathcal{P}$ are translates of each other where the vectors of translation form a lattice, $\mathcal{P}$ is known as a *Bravais lattice* (or, simply, *lattice) packing*. Furthermore, if $\mathcal{P}$ can be decomposed into the union of two distinct lattice packings $\mathcal{P}_0$ and $\mathcal{P}_1$, such that an inversion about some point in the plane interchanges $\mathcal{P}_0$ and $\mathcal{P}_1$, then $\mathcal{P}$ is called a *double-lattice packing*. Generally, if one can decompose $\mathcal{P}$ into the union of $N \geq 1$ distinct lattice packings, each sharing the same lattice vectors, then $\mathcal{P}$ is said to be a *periodic packing* with an *N-particle basis*. Also, for all periodic packings, there exists a fundamental cell (FC) of the packing, parallelogrammatic in shape, described by a lattice matrix $\boldsymbol{\Lambda} = \{\boldsymbol{\lambda}_1, \boldsymbol{\lambda}_2\}$, inside which all N centroids lie. Examples of lattice and periodic packings are given in Figure 1. Note that, in a lattice packing, all particles must have the same orientation, whereas, in a general periodic packing, the N particles in the FC are free to have their own orientations.

The packing density, ϕ, defined for a given $\mathcal{P}$ is, intuitively speaking, the fraction of the plane covered by the copies of S. When it is assumed that $\mathcal{P}$ is a periodic packing with an N-particle basis,

$$\phi = \frac{Na_1}{\text{Area}(F)} \tag{1}$$

, where a_1 denotes the area of a single particle, and Area(F) denotes the area of the FC. If $\phi = 1$, then $\mathcal{P}$ is said to be a *tiling*.

III. TORQUATO-JIAO ADAPTIVE SHRINKING CELL (ASC) OPTIMIZATION SCHEME

The Torquato-Jiao Adaptive Shrinking Cell (ASC) optimization scheme seeks to generate dense packings of a

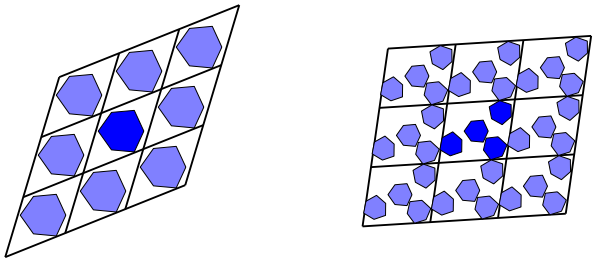

(a) (b)

FIG. 1: (Color online) Examples of a lattice packing (a) and periodic packing with four-particle basis (b). The lattice parallelogram is shown by the black grid behind the particles.

collection of shapes within a periodic FC through a process of rearranging the positions of the shapes within an FC while decreasing the FC's volume in order to increase the packing density. Formally stated, the ASC optimization scheme is

$$\begin{aligned} &\text{minimize } -\phi(\boldsymbol{r}_1^\lambda, \boldsymbol{r}_2^\lambda, \boldsymbol{r}_3^\lambda, \ldots, \boldsymbol{r}_N^\lambda; \theta_1, \theta_2, \theta_3, \ldots, \theta_N; \boldsymbol{\Lambda}), \\ &\text{such that } (S_i \cap S_j) \subseteq (\Gamma_i \cup \Gamma_j) \ \forall i, j = 1, 2, 3, \ldots, N, \\ &\quad i \neq j, \end{aligned} \tag{2}$$

where N is the number of particles in the FC, and $\boldsymbol{r}_i^\lambda$ and θ_i specify the position and orientation of particle i, respectively (see below). The optimization scheme can be solved using a variety of techniques including stochastic search methods with simulated annealing [30, 31] and linear programming [32]; the present work uses an adaptation of the former. For the sake of completeness, the technique will be described here.

In $\mathbb{R}^2$, the ASC scheme utilizes a parallelogrammatic fundamental unit cell (FC) with periodic boundary conditions. The positions of the N particles are given by the lattice coordinates (i.e., the relative coordinates with respect to the lattice vectors) of their centroids, $\boldsymbol{r}_1^\lambda, \boldsymbol{r}_2^\lambda, \boldsymbol{r}_3^\lambda, \ldots \boldsymbol{r}_N^\lambda \in [0, 1)^2$; and (global) orientations, $\theta_1, \theta_2, \theta_3, \ldots, \theta_N \in [0, 2\pi)$. From the initial configuration, the stochastic search method uses an iterative process to increase the packing density. Its main steps are the following:

- Random rotations or translations are applied to the shapes, accepting moves that satisfy the required nonoverlap constraints between the shapes ("random movements"), then
- Random strains, composed of a combination of a deformation and either a dilation or a compression, are applied to the FC that seek to either increase or decrease its area with a specified probability, corresponding to uphill and downhill moves, respectively ("random strains").

During the "random movements" step, every particle in the basis is either translated or rotated within some prescribed limits on the magnitude of the movement. If the new position of the particle does not cause it to overlap with any other particles in the FC (or their periodic images), the move is kept; otherwise, the move is rejected and the particle remains where it began. Note that only one particle is moved at a time; collections of particles never move simultaneously during this step. The process is repeated a specified number of times for each particle to explore the configurational space of the packing; the precise number is determined empirically based on the criterion that the particles are allowed to equilibrate before attempting to strain the FC. In the present work, at least 500 trial movements are attempted for each particle at each occurrence of this step, and this number remains constant for the duration of the simulation.

During the "random strains" step, the simulation box is simultaneously deformed and compressed or dilated in a way that attempts to decrease its area on average while preserving the nonoverlap constraints. Since the locations of the particles are expressed in terms of the lattice vectors, straining the simulation box also effects a collective motion of the particles. The straining process is attempted up to a prescribed maximum number of attempts. The first successful strain is kept, and the algorithm returns to the first step (random movements). After each unsuccessful strain attempt, the maximum allowed strain is decreased by a constant ratio in order to steadily increase the chances of finding a valid strain. Therefore, more attempts are required as the packing increases in density. In addition, uphill moves that allow the FC to expand are allowed with a given probability.

The maximum magnitude of the trial movements is steadily decreased throughout the execution of the algorithm, reducing the maximum magnitude by a constant ratio when the acceptance rate of trial moves falls significantly below 50%. Moreover, while the maximum strain magnitude is decreased after each unsuccessful attempt, the maximum magnitude is restored to its original value the next time the "random strains" step occurs, since, for example, particle movements within the FC may result in two particles being next to each other at the end of one "random movements" step (necessitating a small strain), and may result in the particles being more uniformly spaced at the end of the next step (allowing for a larger strain even though the FC may be smaller).

The sequence of random movements and random strains is repeated a prescribed number of times, chosen such that the algorithm has "enough time" to find and settle in a minimum of the objective function (which is determined by monitoring the convergence of the packing density); in the present work, the maximum number of iterations is always at least 500. In order to refine the results, a "fine tuning" procedure may be used in which the ASC algorithm is executed a second time, starting with the previous final dense configuration by expanding the FC by some small amount and greatly reducing the

magnitude of the movements and strains in order to more accurately approach the density maximum that has been identified. However, this process is only used in cases where the particles are convex, since this is necessary to ensure that a general expansion of the FC does not introduce overlaps.

In the past, the ASC scheme has been applied to determining packings of convex polyhedra in three and higher dimensions, detecting overlaps between particles through use of the separation axis theorem [30, 31]; in this work, the algorithm has been modified to detect overlaps between concave particles in two dimensions through a combinatoric check of the particle's edges, which may be some combination of line segments and circular arc segments.

This solution of the ASC scheme is a particularly strong investigative tool since it is capable of identifying dense packing configurations quickly and with appreciable consistency. Analytical methods may then be used, benefitting from the information derived from the algorithm's results to determine the exact structures of the packings. In addition, the freedom to choose any initial condition may be used to enhance the quality of solutions found if an interesting structure is more often realized through specific initial conditions [32]. In the present work, we find that, by choosing initial lattice vectors that more closely resemble the final lattice vectors of dense structures, denser results are achieved, and with increased frequency.

IV. NONCIRCULAR PARTICLE SHAPES

A variety of noncircular particle shapes were studied in the present work; this section aims to make precise the geometries that were studied. In order to establish benchmarks for the program's performance, the well-known cases of regular pentagons and octagons were considered. In addition, we consider three families of nontrivial particle shapes: "fat crosses", "curved triangles", and "moon-like shapes". The packing characteristics of these noncircular particle shapes have heretofore not been studied. We show that they lead to unique packing arrangements.

A. Fat Cross

The first nontrivial particle shape that we investigate is a so-called "fat cross." Several examples of this particle shape are given in Figure 2. The particle shape is described by a width parameter w according to the definition

$$w = \frac{\delta}{l}, \tag{3}$$

where δ is the width of the cross's legs, and l is the end-to-end length of the cross. Therefore, it follows that $w \in [0, 1]$; the $w = 0$ case corresponds to a pair of lines of length l bisecting each other at a right angle, and the $w = 1$ case corresponds to a square of side length l.

B. Curved Triangle

Another particle shape that we investigate is the so-called "curved triangle," that, in the convex case, is a two-dimensional analog of the "tetrahedral puff" described in [34]. This particle shape is derived by replacing the sides of an equilateral triangle with circular arc segments; this is illustrated in Figure 3. The particle shape may then described by a parameter

$$k = \pm\frac{r_0}{r}, \tag{4}$$

where r is the radius of the arc segments, and r_0 is the radius of a circle passing through the triangle's vertices. k is taken by convention to be positive when the curved triangle is convex as in Figure 3a, and negative when the curved triangle is concave as in Figure 3b. When $k = 0$, then the particle shape becomes an equilateral triangle; when $k = 1/\sqrt{3} = 0.577350\ldots$, the particle shape becomes the well-known Reuleaux triangle [35]; and when $k = 1$, the particle shape becomes a circle. When $k = -1/\sqrt{3}$, the vertices of the particle become cusps, and in order to decrease k beyond this point, a line segment connects the cusp and the vertex, as is shown in Figure 3c; the curved triangle is said to be "spiked" in this regime, and begins to resemble the Mercedes-Benz logo. In the limit $k \to -\infty$, the particle shape becomes the union of three line segments of length r_0, each at an angle of $2\pi/3$ from the others.

C. Moon-Like Shape

The third nontrivial particle shape that we investigate is the a "moon-like" shape, which is constructed by a pair of circular arc segments with radii r_0 and r, where the former arc is a half-circle. The particle shape is parameterized by the same parameter k used to characterize the curved triangle [cf. Eq. (4)], where k is, by convention, taken to be negative when the particle shape is a concave, "crescent" shape, as in Figure 4a and positive when the moon is a convex, "gibbous" shape, as in Figure 4b.

V. RESULTS

The stochastic search solution of the ASC scheme described in Sec. III is used to generate dense periodic packings of congruent copies of the particle shapes described above, and the resulting computer-generated packings are used to inform analytical predictions for the structures of the densest packings; the following details the results of the numerical simulations and discusses

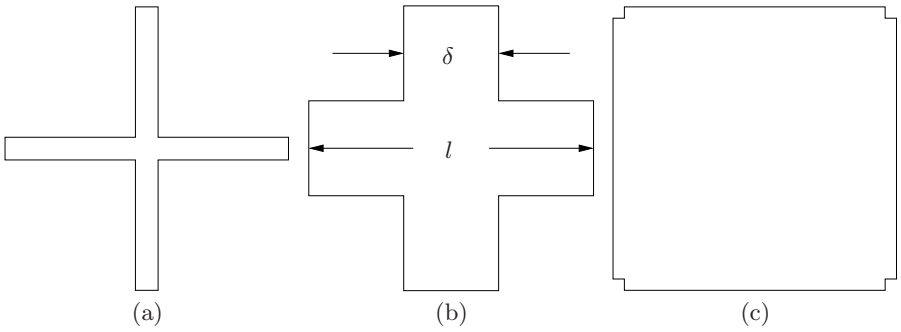

FIG. 2: Three instances of the general "fat cross" with $w = 1/10$ (a), $1/3$ (b), and $9/10$ (c).

the structures that we find. We also provide visual representations of some noteworthy cases. A summary of the densest packing behavior of the noncircular particle shapes the we obtain is given in Table I.

A. Octagons

Periodic packings of congruent copies of regular octagons were generated using the ASC algorithm with one-, two-, three-, and four-particle bases. Some noteworthy computer-generated packings are shown in Figure 5. The ASC algorithm finds periodic packings of octagons in accordance with Fejes Tóth's well-known theorem that the densest packing of a centrally-symmetric convex particle shape is realized by a lattice packing [18]. Moreover, the packing densities found via numerical simulation are remarkably close to the theoretical optimum: $\delta\phi_1 = 2.0 \times 10^{-5}$, $\delta\phi_2 = 1.35 \times 10^{-4}$, $\delta\phi_3 = 2.35 \times 10^{-4}$, and $\delta\phi_4 = 2.61 \times 10^{-4}$, where $\delta\phi_N$ denotes the difference in packing density between the analytical optimal construction and the best numerical result using an N-particle basis.

B. Pentagons

Periodic packings of congruent copies of regular pentagons were generated using the ASC algorithm with two- and four-particle bases. Figure 6 shows some noteworthy numerical findings. These results closely resemble the best-known packing of pentagons, whose packing density is $\phi = (5 - \sqrt{5})/3 = 0.921311\ldots$; the packings shown in Figures 6a and 6b differed from this by 2.09×10^{-4} and 1.0×10^{-5}, respectively. These packings show the structure conjectured to be the densest packing of pentagons [24–27]. Indeed, it is conjectured that, for a wide class of bodies lacking central symmetry, the densest packing is realized in a double-lattice configuration. The regular pentagon is one of these shapes.

C. Fat Crosses

Periodic packings of congruent copies of fat crosses were generated using the ASC algorithm with four-particle bases for various values of w. From these simulations, four different packing behaviors were observed. Figure 7 compares the packing density of a number of computer-generated cases against the analytical putative maximum packing density. The curve contains four piecewise-smooth regimes, corresponding to four different structures, identified as L_1, L_2, L_3, and L_4, in order of increasing w. Figure 8 shows a few selected packings to show these different configurations. Notice that at $w = 1/3, 1/2,$ and 1, the packing becomes a tiling. It is interesting to note that, though this shape is concave, all of the densest packings found are lattice packings. Another interesting property of these packings is that, in the limit case $w = 0$, the fat cross is equivalent (up to a scaling constant) to the limit case of a superdisk, $\lim_{p\to 0}\{(x, y) \in \mathbb{R}^2 : |x|^{2p} + |y|^{2p} \leq 1\}$, and the analytical packing structure matches this superdisk's already-known densest packing [36]. The fat crosses' putative maximum packing density is tabulated for several representative values in Table II; see the *Supplemental Material* for mathematical details about the various packing structures.

D. Curved Triangles

Periodic packings of congruent copies of convex curved triangles were generated using the ASC algorithm with two- and four-particle bases for various values of k. Using a method of Kuperberg and Kuperberg [25], the densest double-lattice packing of convex curved triangles was derived as a function of the curvature parameter k. This function is plotted as a solid curve in Figure 9, and computer-generated packings with a two-particle basis are plotted as triangular marks; it was observed that the results predicted by the Monte Carlo method using a two-particle basis closely matched the optimal double-lattice packing for all of the chosen values of k.

Figures 10 and 11 show a few of the packings that

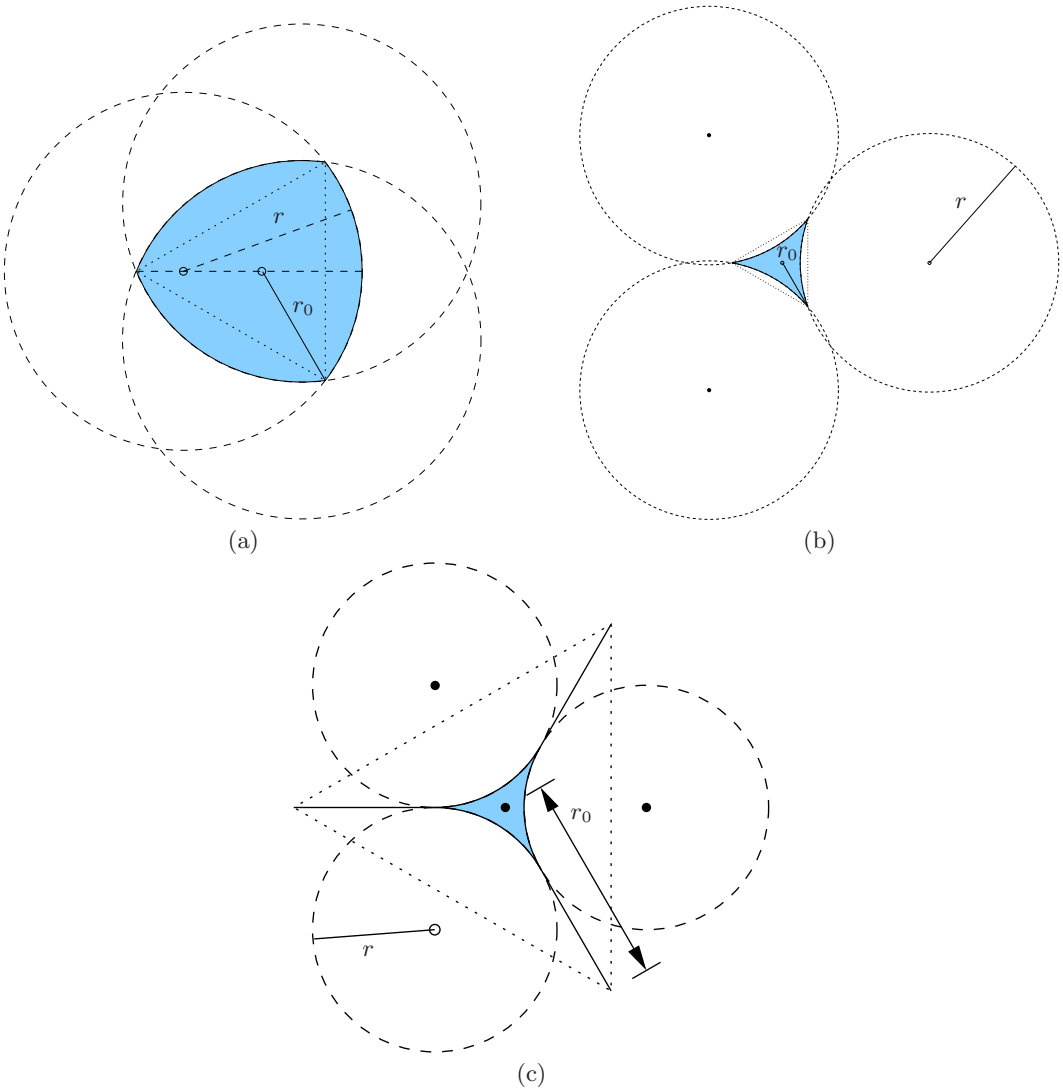

FIG. 3: (Color online) Three examples of the basic form of a curved triangle: convex ((a), $k = 0.71$), concave ((b), $k = -0.39$), and "spiked" ((c), $k = -1.55$).

TABLE I: Symmetries of the putative densest packings of the aforementioned particle shapes. The properties of well-known shapes (pentagons and octagons) are compared to the results we obtain for our nontrivial particle shapes (fat crosses, curved triangles, and moon-like shapes).

Shape Name	Convex	Centrally-Symmetric Particle	Centrally-Symmetric Basis	N
Pentagon	Yes	No	Yes	2
Octagon	Yes	Yes	Yes	1
Fat Cross	No	Yes	Yes	1
Curved Triangle	depends on k	No	Yes	2,4 (depending on k)
Moon-like shape	depends on k	No	depends on k	2

were generated by the ASC algorithm with two- and four-particle bases, respectively. Notice that the densest packings with a two-particle basis are double-lattice packings, implying a centrally-symmetric basis. However, in all of the cases where $0 < k < 1/\sqrt{3}$, it was observed that the triangles do *not* line up such that their vertices touch. Instead, the two adjacent triangles are rotated slightly so that the vertex of one contacts the arc of the other. Indeed, when determining the optimal double-lattice structure by a method of Kuperberg and Kuperberg [25], it

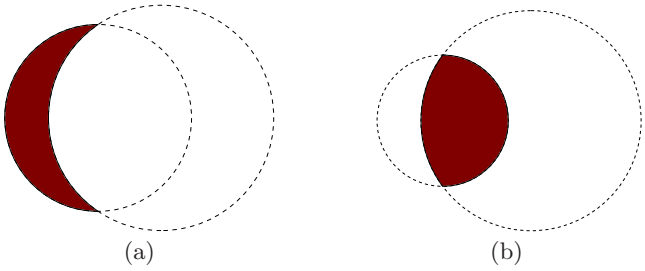

(a) (b)

FIG. 4: (Color online) Examples of a "crescent" ((a), $k > 0$) and a "gibbous" ((b), $k < 0$) moon-like shape, .

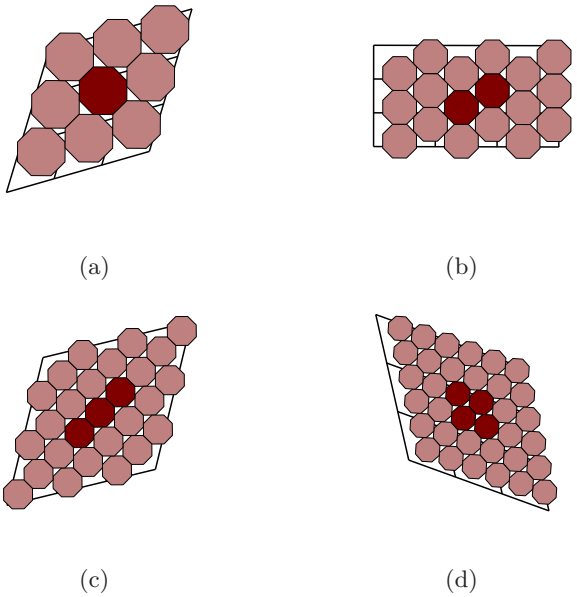

(a) (b)

(c) (d)

FIG. 5: (Color online) Computer-generated dense periodic packings of octagons using one- (a), two- (b), three- (c), and four-particle (d) bases. The packing densities are $\phi = 0.906144$, 0.906029, 0.905929, and 0.905903, respectively

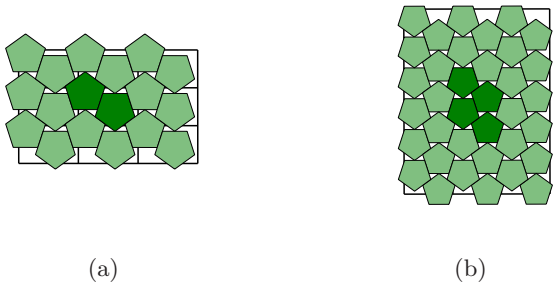

(a) (b)

FIG. 6: (Color online) Computer-generated dense periodic packings of pentagons using two- (a) and four-particle (b) bases. The packing densities are $\phi = 0.921102$ and 0.921301, respectively.

was found that this small perturbation actually increases

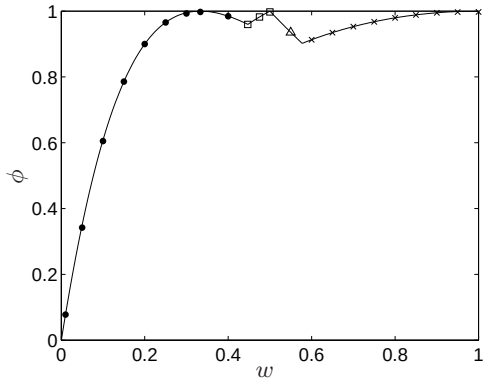

FIG. 7: Analytically-derived (solid curve) and computer-generated (data points) packing densities for packings of fat crosses as a function of width parameter w. The structures are labeled as follows: filled circle = L_1, square = L_2, triangle = L_3, cross = L_4.

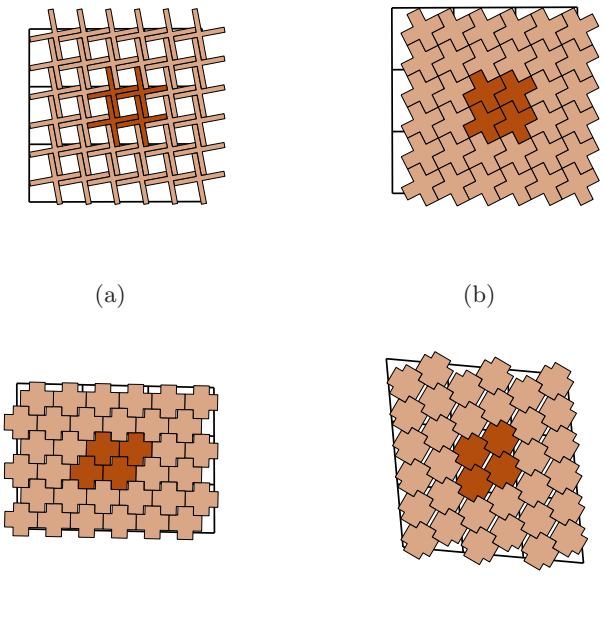

(a) (b)

(d) (e)

FIG. 8: (Color online) Computer-generated dense periodic packings of fat crosses for various values of w showing the four structures observed. The L_1 structure is shown for $w = 1/10$ (a), 1/3 (b), and 2/5 (c); the L_2 structure is shown for $w = 19/40$ (d); the L_3 structure is shown for $w = 11/20$ (e); and the L_4 structure is shown for $w = 7/10$ (f).

the packing density when $0 < k < 1/\sqrt{3}$, meaning that this characteristic of the numerical results is not due to numerical inaccuracies, but, on the contrary, showcases the sensitivity of the stochastic search in finding dense packings.

TABLE II: Putative maximum packing densities of congruent copies of fat crosses for selected values of w.

w	$\phi(w)$
0.1	$76/125 = 0.608$
0.2	$9/10$
0.3	$204/205 = 0.995121\ldots$
0.4	$64/65 = 0.984615\ldots$
0.48	$912/925 = 0.985945\ldots$
0.55	$29/31 = 0.935483\ldots$
0.6	$21/23 = 0.913043\ldots$
0.7	$182/191 = 0.952879\ldots$
0.8	$48/49 = 0.979591\ldots$
0.9	$198/199 = 0.994974\ldots$

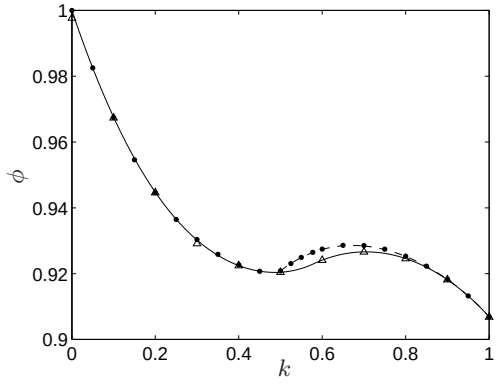

FIG. 9: Analytically-derived and computer-generated packing densities of curved triangles for various values of k. The solid curve denotes the density of the optimal double lattice packing, and the dashed curve shows the density of the optimal periodic packing with a four-particle basis; triangle and filled circle data points denote densities obtained by computer-generated packings with two- and four-particle bases, respectively.

(a) (b)

FIG. 10: (Color online) Computer-generated dense periodic packings of curved triangles with a two-particle basis for $k = 2/5$ (a) and $4/5$ (b); $\phi = 0.922437$ and 0.924589, respectively.

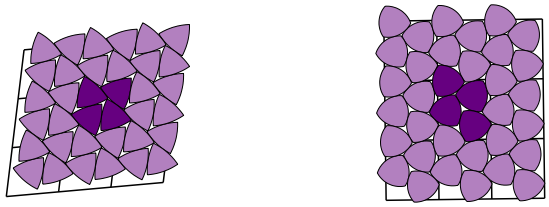

(a) (b)

FIG. 11: (Color online) Computer-generated dense periodic packings of curved triangles with a four-particle basis for $k = 3/10$ (a) and $7/10$ (b); $\phi = 0.921528$ and 0.921460, respectively.

Numerical results using a four-particle basis showed that, for sufficiently large k, a packing structure exists whose density is significantly higher than the best double-lattice packing; below this point, the four-particle basis' optimal configuration is a degenerate case of the two-particle basis, as shown in Figure 11a; an example of the non-degenerate four-particle basis structure is given in Figure 11b. Numerical results using an eight-particle basis, an example of which is shown in Figure 12, provide additional evidence that the four-particle basis is in fact the densest configuration. These results were verified by determining the analytical structure of the four-particle basis that is currently the best-known packing structure for this shape. The densities of computer-generated packings of curved triangles using a four-particle basis are plotted as filled circles, and the corresponding analytical packing density is displayed as a dashed line in Figure 9. Though periodic tilings of convex particles have been shown that exhibit more than a two-particle basis [37–39], we do not know of any other convex, non-tiling shapes that have been observed to exhibit this behavior [40].

In order to create this four-particle packing structure, the particles in the FC, denoted A_0, B_0, C_0, and D_0, are placed facing straight-up and straight-down, where particles A_0 and D_0 are both in contact with all of the other particles in the basis, as shown in Figure 13. The lattice vectors $\boldsymbol{\lambda}_1$ and $\boldsymbol{\lambda}_2$ are found by finding the positions of shapes A_1 and A_2 (both of which are periodic images of A_0) relative to A_0. All of the bodies in the basis are rotated by the same angle θ: A and D are rotated anti-clockwise, and B and C are rotated clockwise. Doing this causes B_1 and C_2 (and their periodic images) to come into contact. Once this contact is established, the packing achieves its maximum density; this result is shown in Figure 14. The curved triangles' putative maximum packing density is tabulated for some representative values of k in Table III; see the *Supplemental Material* for details of the analytical construction of this packing. In addition, computer-generated packings of *concave* curved triangles are provided in the Appendix without analytical

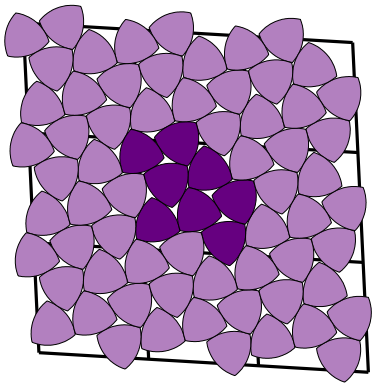

FIG. 12: (Color online) A computer-generated densest packing of curved triangles with an eight-particle basis ($k = 0.62$), showing a structure that is a degenerate case of the best-known four-particle basis.

constructions; all of these packings appear to be double-lattice packings.

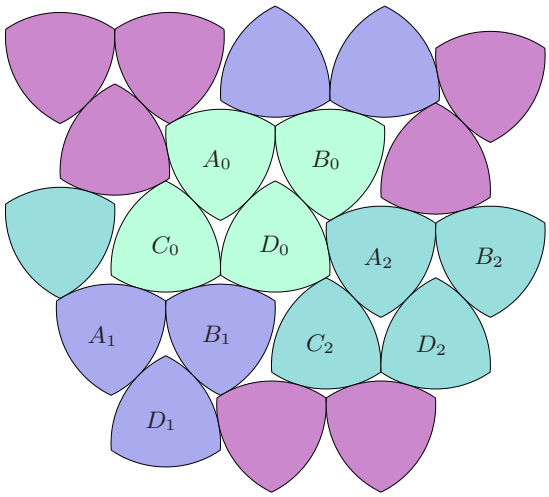

FIG. 13: (Color online) A portion of the analytical packing without any applied rotation ($k = 0.65$). Notice that a gap exists between B_1 and C_2 (and their periodic images). Applying the rotation closes this gap and maximizes the packing density.

E. Moon-like Shapes

Periodic packings of congruent copies of moon-like shapes were generated using the ASC algorithm with two- and four-particle bases for various values of k. The densest computer generated packings are plotted as data points along solid curves denoting three different analytical constructions in Figure 15. The first structure observed was a double-lattice packing shown in Figures 16a and 16d. This structure is indicated in Figure 15 by triangular data points and will be referred to as the D_1 structure. The second structure observed was a non-double-lattice periodic packing with a two-particle basis, shown in Figure 16b; it is indicated in Figure 15 by square data points and will be referred to as the B-structure. The third structure observed was a second double-lattice packing, shown in Figure 16c. This structure is indicated in Figure 15 by filled circle data points and is denoted as the D_2-structure. The putative densest packings of moon-like shapes are tabulated as a function of k in Table IV.

The B-structure is a unique structure in that its fundamental basis possesses no inherent symmetries. Furthermore, its discovery underscores the utility of the ASC algorithm in determining the densest packings that are not obvious by inspection.

TABLE III: Putative maximum packing densities of congruent copies of convex curved triangles for selected values of k.

k	$\phi(k)$
0.1	0.967582 . . .
0.2	0.944761 . . .
0.3	0.930217 . . .
0.4	0.922458 . . .
0.5	0.922458 . . .
0.6	0.927362 . . .
0.7	0.928415 . . .
0.8	0.925249 . . .
0.9	0.918262 . . .

TABLE IV: Putative maximum packing densities of congruent copies of moon-like shapes for selected values of k.

k	$\phi(k)$	k	$\phi(k)$
−0.9	0.928125 . . .	0.1	0.936131 . . .
−0.8	0.916116 . . .	0.2	0.935451 . . .
−0.7	0.910371 . . .	0.3	0.933966 . . .
−0.6	0.907259 . . .	0.4	0.931709 . . .
−0.5	0.911837 . . .	0.5	0.928675 . . .
−0.4	0.921385 . . .	0.6	0.924819 . . .
−0.3	0.928392 . . .	0.7	0.920053 . . .
−0.2	0.932303 . . .	0.8	0.915055 . . .
−0.1	0.933906 . . .	0.9	0.914783 . . .
0	0.935931 . . .	0.95	0.913563 . . .

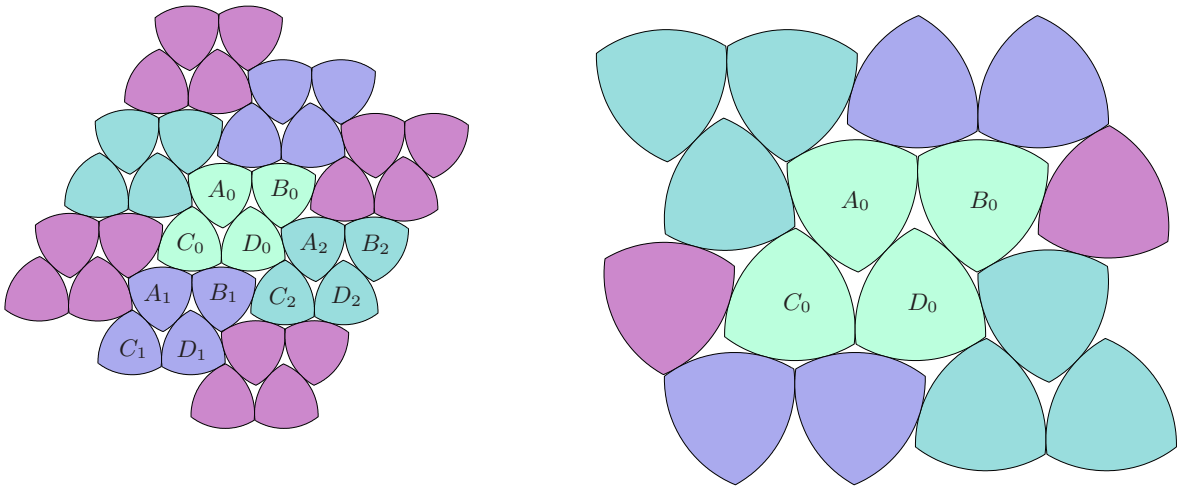

(a) (b)

FIG. 14: (Color online) The analytically-derived packing of curved triangles ($k = 0.65$) with the applied rotation (a); a zoomed-in view is provided in (b). Triangles A_0 and D_0 are rotated anti-clockwise by θ, and triangles B and C are rotated clockwise by θ, where $\theta = 0.057$ rad. $\phi = 0.928473\ldots$.

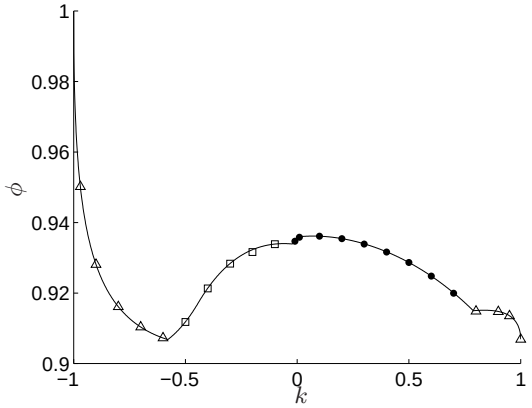

FIG. 15: Putative maximum packing densities for congruent copies of moon-like shapes as a function of k. The three different structures are denoted as follows: triangle = D_1, square = B, dot = D_2); the solid curve shows the analytical densities.

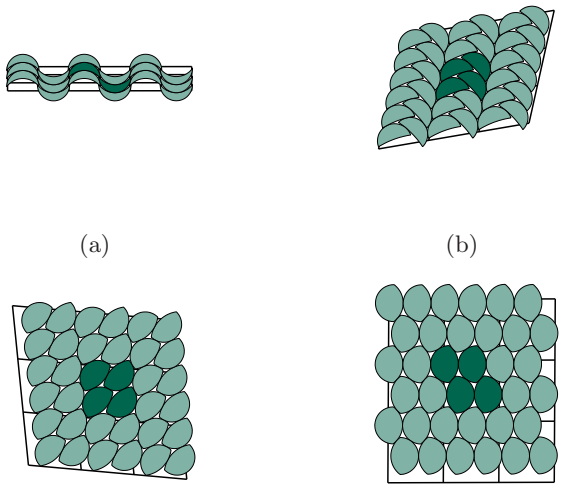

FIG. 16: (Color online) Computer-generated dense periodic packings of moon-like shapes for various values of k, displaying the three different packing structures observed. (a): $k = -0.8$ (D_1-structure, crescent instance). (b): $k = -0.2$ (B-structure). (c): $k = 0.6$ (D_2-structure). (d): $k = 0.9$ (D_1-structure, gibbous instance).

VI. CONCLUSIONS AND FUTURE WORK

In this paper, we implemented a two-dimensional implementation of the Torquato-Jiao Adaptive Shrinking Cell scheme using a stochastic search with simulated annealing to study the dense packing behavior of a variety of well-known and nontrivial particle shapes. We confirmed the utility of the algorithm by reproducing the well-known densest packings of regular pentagons and octagons. Next, we applied the algorithm to several nontrivial particle shapes to find their densest packing behavior. It is especially worth noting that the ASC scheme correctly and accurately predicted subtle perturbations in the two-particle packings of curved triangles that are not immediately intuitively apparent.

The packing characteristics of the curved triangle

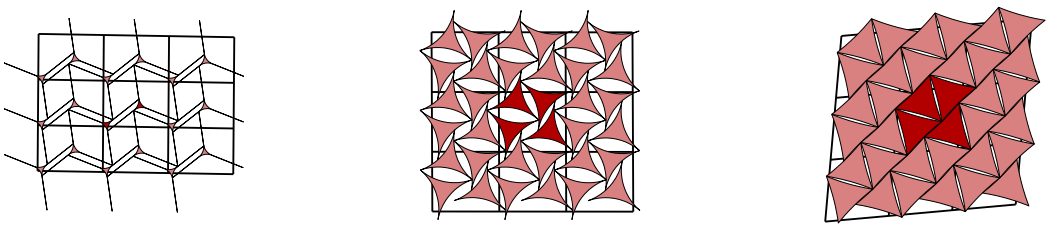

(a) (b) (c)

FIG. 17: (Color online) Computer-generated dense periodic packings of concave curved triangles for $k' = 1/20$ (a), 27/100 (b), and 9/20 (c). The packing densities are $\phi = 0.019141$, 0.446702, and 0.896363, respectively. All of these packing suggest double-lattice structures.

shape class are unlike anything studied before because its optimal packing density is *not* achieved using a double-lattice packing for sufficiently high curvature. In addition, the B-structure that achieves the densest packings of certain moon-like shapes is a counterintuitive finding for its lack of symmetry in its fundamental basis. These discoveries underscore the utility of the stochastic search implementation of the ASC scheme because of its ability to accurately predict these structures up to the small details inherent in them.

The packing structures discussed in this work offer insights towards the organizing principles for three-dimensional particles in Ref. [1]. For example, the densest packings of regular polygons, as two-dimensional analogs of convex polyhedra, show similar behavior in that the densest packings of regular polygons possessing central symmetry are given by their corresponding densest lattice packings; and the densest packings of those lacking central symmetry are nonetheless given by packings that possess a point of inversion symmetry. Furthermore, the densest packings of fat crosses are given by their corresponding densest lattice packings, in much the same way that the densest packings of three-dimensional, centrally-symmetric polyhedra are conjectured to be given by their corresponding densest lattice packings. One final interesting remark is that the B structure of moon-like shapes possesses no points of inversion. This is in contrast to the proposition in three dimensions that the densest packings of concave polyhedral particles are composed of centrally symmetric compound units. It seems intuitively true that, by approximating the appropriate moon-like shape as a polygon with sufficiently many edges, some structure similar to B structure will achieve the densest packing (which has no points of inversion).

It will be desirable in future work to determine the analytical packing behavior of the concave instance of the curved triangle (for which computer-generated results are provided in the Appendix) for the sake of completeness. More generally, the algorithm used in this work may be adapted to generate both packings of hard particles in closed containers. By altering the shrinking behavior of the domain, it may be possible to study both densest packings and disordered jammed packings. Furthermore, the algorithm may be readily adapted to study packings of particles with a polydispersity in size and shape. Finally, the stochastic search solution to the ASC scheme may readily be adapted to investigate the dense packing behavior of concave solids in higher dimensions.

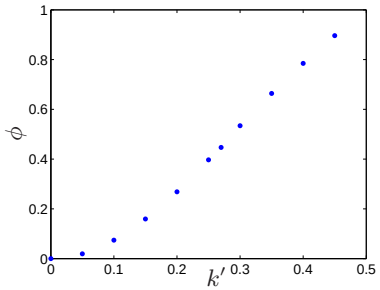

FIG. 18: (Color online) Densities of computer generated packings of concave curved triangles for various values of k'.

ACKNOWLEDGEMENTS

This work was supported by the Materials Research Science and Engineering Center (MRSEC) Program of the National Science Foundation under Grant No. DMR-0820341 and by the Division of Mathematical Sciences at the National Science Foundation under Award Number DMS-1211087.

APPENDIX: MAXIMALLY DENSE PACKINGS OF TWO-DIMENSIONAL CONVEX AND CONCAVE NONCIRCULAR PARTICLES

Figure 17 shows a collection of computer-generated dense periodic packings of *concave* curved triangles with two- and four-particle bases. A double-lattice structure was observed for all particle shapes that we tried. The packing densities of the computer-generated cases are plotted in Figure 18 as a function of an alternative parameter k', defined as the ratio of the inradius of the particle to its circumradius. According to this alternative parameter, the $k' = 0$ limit is equivalent to the $k = -\infty$ limit (Mercedes-Benz limit), and $k' = 1/2$ describes an equilateral triangle ($k = 0$).

[1] S. Torquato and Y. Jiao, Phys. Rev. E **86**, 011102 (2012).
[2] J. D. Bernal, "Liquids: Structure, properties, solid interactions," (Elsevier, Amsterdam, 1965) pp. 25–50.
[3] R. Zallen, *The Physics of Amorphous Solids* (Wiley, New York, 2005).
[4] S. Torquato, *Random Heterogeneous Materials: Microstructure and Macroscopic Properties* (Springer-Verlag, New York, 2002).
[5] P. Chaikin and T. Lubensky, *Principles of Condensed Matter Physics* (Cambridge University Press, 2000).
[6] P. Corradini, V. Petraccone, and B. Pirozzi, European Polymer Journal **19**, 299 (1983).
[7] T. Yamaguchi, T. Asada, H. Hayashi, and N. Nakamura, Macromolecules **22**, 1141 (1989)..
[8] J. Liang and K. A. Dill, Biophysical Journal **81**, 751 (2001).
[9] P. K. Purohit, J. Kondev, and R. Phillips, Proc. Natl. Acad. Sci. USA **100**, 3173 (2003).
[10] J. L. Gevertz and S. Torquato, PLoS Comput Biol **4**, e1000152 (2008).
[11] M. Ohring, *Materials Science of Thin Films* (Academic Press, 2001).
[12] W. Azzam, P. Cyganik, G. Witte, M. Buck, and C. Wll, Langmuir **19**, 8262 (2003)..
[13] P. Cyganik, M. Buck, W. Azzam, and C. Wll, The Journal of Physical Chemistry B **108**, 4989 (2004)..
[14] R. Farhadifar, J.-C. Rper, B. Aigouy, S. Eaton, and F. Jlicher, Current Biology **17**, 2095 (2007).
[15] A.-K. Classen, K. I. Anderson, E. Marois, and S. Eaton, journal Developmental Cell **9**, 805 (2005).
[16] C. A. Rogers, *Packing and Covering* (Cambridge University Press, 1964).
[17] C. A. Rogers, Acta Math **86**, 309 (1951).
[18] L. Fejes Tóth, Acta Sci. Math. **12A**, 62 (1950).
[19] B. Grünbaum and G. Shephard, Bull. Amer. Math Soc. **3**, 951 (1980).
[20] J. H. Conway and J. Lagarias, Journal of Combinatorial Theory, Series A **53**, 183 (1990).
[21] J. H. Conway and K. M. Knowles, Journal of Physics A: Mathematical and General **19**, 3645 (1986).
[22] L. Fejes Tóth, *Regular Figures* (MacMillan, New York, 1964).
[23] K. Reinhardt, Abh. Math. Sem. Hamburg **10**, 216 (1934).
[24] C. L. Henley, Phys. Rev. B **34**, 797 (1986).
[25] G. Kuperberg and W. Kuperberg, Discrete & Computational Geometry **5**, 389 (1990), 10.1007/BF02187800.
[26] Y. L. Duparcmeur, A. Gervois, and J. P. Troadec, Journal of Physics: Condensed Matter **7**, 3421 (1995).
[27] T. Schilling, S. Pronk, B. Mulder, and D. Frenkel, Phys. Rev. E **71**, 036138 (2005).
[28] L. Fejes Tóth, Proc. Kon. Ned. Aka. Wet. **51**, 189 (1948).
[29] K. Mahler, Duke Math J. **13**, 611 (1946).
[30] S. Torquato and Y. Jiao, Nature **460**, 876 (2009).
[31] S. Torquato and Y. Jiao, Phys. Rev. E **80**, 041104 (2009).
[32] S. Torquato and Y. Jiao, Phys. Rev. E **82**, 061302 (2010).
[33] See Supplemental Material at `http://link.aps.org/supplemental/10.1103/PhysRevE.86.031302` for mathematical details for the packing structures presented in this paper.
[34] Y. Kallus and V. Elser, Phys. Rev. E **83**, 036703 (2011).
[35] F. Reuleaux, *Kinematics of Machinery; Outlines of a Theory of Machines*, edited by A. Kennedy (MacMillan, London, 1875).
[36] Y. Jiao, F. H. Stillinger, and S. Torquato, Phys. Rev. Lett. **100**, 245504 (2008).
[37] K. Reinhardt, *Über die Zerlegung der Ebene in Polygone*, Ph.D. thesis, Königlichen Universität zu Frankfurt (1918).
[38] R. B. Kershner, The American Mathematical Monthly **75**, pp. 839 (1968).
[39] H. Heesch, *Reguläres Parkettierungsproblem* (Westdeutscher Verlag, 1968).
[40] We do not consider particle shapes derived from applying trivial perturbations (that is, those that do not alter the densest packing structure) to shapes that form tilings.